Atomic Layer Deposition of Molybdenum Nitride from Bis(*tert*-butylimido)-bis(dimethylamido)molybdenum and Ammonia onto Several Types of Substrate Materials with Equal Growth per Cycle

Ville Miikkulainen, Mika Suvanto, and Tapani A. Pakkanen*

Department of Chemistry, University of Joensuu, P.O. Box 111, FIN-80101 Joensuu, Finland

Received August 28, 2006. Revised Manuscript Received October 19, 2006

Atomic layer deposition (ALD) was used to deposit thin films of molybdenum nitride from a new precursor, bis(*tert*-butylimido)-bis(dimethylamido)molybdenum, and ammonia. The optimum ALD growth window was 260−300 °C and the maximum growth per cycle 0.5 Å. Deposition temperatures are lower than with the previously reported molybdenum pentachloride as the precursor. Molybdenum nitride was successfully deposited on silicon, electrochemically grown nickel, chromium, and quartz glass. Growth per cycle was maintained over substrate materials of different types. Conformality of the deposited films was as high as 98%. Films were mainly amorphous, containing small amounts of the β-Mo_2N phase. According to time-of-flight elastic recoil detection analysis (TOF-ERDA), the molybdenum−nitrogen ratio was close one. Together with X-ray diffraction data this suggests the existence of a nitrogen-rich amorphous phase in the film.

Introduction

Among their several favorable properties, thin films of transition metal nitrides have good mechanical and chemical stability, a low coefficient of friction, and good hardness.[1] Titanium nitride has been of particular interest, both in research and for industrial applications.[2−6] Nitrides of other transition metals have attracted much less attention. Molybdenum nitride has been studied for applications as catalyst,[7−15] a diffusion barrier in microelectronics,[16] high-T_c superconductors,[17−19] and tribological coatings.[20−24] For cubic stoichiometric MoN, the critical temperature for superconductivity has been predicted to be as high as 29.4 K[25]. The synthesis of the cubic phase MoN has not been reported. The bulk modulus of hexagonal δ-MoN phase is the highest of any known compound material.[26,27]

Atomic layer deposition (ALD), formerly known as atomic layer epitaxy (ALE), is a method of thin film deposition developed in the 1970s by Suntola and Antson.[28] In ALD, vapors of precursors are alternately pulsed into the reactor space and onto the substrate surface. On the substrate, precursor molecules react chemically with chemically active surface groups such as hydroxyls. Between source pulses the reactor chamber is purged with inert gas, which prevents undesirable gas-phase reactions.[29] With suitable process parameters the film growth is self-limiting, which means that thin films can be constructed layer-by-layer. ALD has many unique features, including accurate control of film thickness, excellent conformality, and reproducibility of high quality thin films. The main applications of ALD are in microelec-

* To whom correspondence should be addressed. E-mail: tapani.pakkanen@joensuu.fi.

(1) Lengauer, W. In *Transition Metal Carbides, Nitrides and Carbonitrides*; Riedel, R., Ed.; Handbook of Ceramic Hard Materials, Vol. 1; Wiley: Weinheim, 2000.
(2) Fix, R.; Gordon, R. G.; Hoffman, D. M. *Chem. Mater.* **1991**, *3*, 1138.
(3) Mitterer, C.; Holler, F.; Reitberger, D.; Badisch, E.; Stoiber, M.; Lugmair, C.; Nöbauer, R.; Müller, Th.; Kullmer, R. *Surf. Coat. Technol.* **2003**, *716*, 163−164.
(4) Molarius, J. M.; Korhonen, A. S.; Ristolainen, E. O. *J. Vac. Sci. Technol., A* **1985**, *3*, 2419.
(5) Hogmark, S.; Jacobson, S.; Larsson, M. *Wear* **2000**, *246*, 20.
(6) Cunha, L.; Andritschky, M.; Pischow, K.; Wang, Z.; Zarychta, A.; Miranda, A. S.; Cunha, A. M. *Surf. Coat. Technol.* **2002**, *153*, 160.
(7) Lee, K. S.; Abe, H.; Reimer, J. A.; Bell, A. T. *J. Catal.* **1993**, *139*, 34.
(8) Kadono, T.; Kubota, T.; Okamoto, Y. *Catal. Today* **2003**, *87*, 107.
(9) Gong, S.; Chen, H.; Li, W.; Li, B. *Catal. Commun.* **2004**, *5*, 621.
(10) Gong, S.; Chen, H.; Li, W.; Li, B.; Hu, T. *J. Mol. Catal. A: Chem.* **2005**, *225*, 213.
(11) Nagai, M.; Yamamoto, Y.; Aono, R. *Colloids Surf., A* **2004**, *241*, 257.
(12) Shi, C.; Zhu, A. M.; Yang, X. F.; Au, C. T. *Appl. Catal., A* **2004**, *276*, 223.
(13) Kojima, R.; Aika, K.-i. *Appl. Catal., A* **2001**, *219*, 141.
(14) Lee, H. J.; Choi, J.-G.; Colling, C. V.; Mudholkar, M. S.; Thompson, L. T. *Appl. Surf. Sci.* **1995**, *89*, 121.
(15) Chen, X.; Zhang, T.; Zheng, M.; Wu, Z.; Wu, W.; Li, C. *J. Catal.* **2004**, *224*, 473.
(16) He, Y.; Feng, J. Y. *J. Cryst. Growth* **2004**, *263*, 203.
(17) Savvides, N. *J. Appl. Phys.* **1987**, *62*, 600.
(18) Bull, C. L.; McMillan, P. F.; Soignard, E.; Leinenweber, K. *J. Solid State Chem.* **2004**, *177*, 1488.
(19) Bezinge, A.; Yvon, K.; Muller, J. *Solid State Commun.* **1987**, *63*, 141.
(20) Danroc, J.; Aubert, A.; Gillet, R. *Thin Solid Films* **1987**, *153*, 281.
(21) Valli, J.; Mäkelä, U.; Hentzell, H. T. G. *J. Vac. Sci. Technol., A* **1986**, *4*, 2850.
(22) Sanjinés, R.; Hones, P.; Lévy, F. *Thin Solid Films* **1998**, *332*, 225.
(23) Lévy, F.; Hones, P.; Schmid, P. E.; Sanjinés, R.; Diserens, M.; Wiemer, C. *Surf. Coat. Technol.* **1999**, *284*, 120−121.
(24) Hones, P.; Martin, N.; Regula, M.; Lévy, F. *J. Phys. D: Appl. Phys.* **2003**, *36*, 1023.
(25) Papaconstantopoulos, D. A.; Pickett, W. E.; Klein, B. M.; Boyer, L. L. *Phys. Rev. B* **1985**, *31*, 752.
(26) Soignard, E.; McMillan, P. F.; Chaplin, T. D.; Farag, S. H.; Bull, C. L.; Somayazulu, M. S.; Leinenweber, K. *Phys. Rev. B* **2003**, *68*, 132101.
(27) McMillan, P. F. *Nat. Mater.* **2002**, *1*, 19.
(28) Suntola, T.; Antson, J. U.S. Patent 4,058,430, 1977.
(29) Suntola, T. *Mater. Sci. Rep.* **1989**, *4*, 261.

10.1021/cm0620279 CCC: $37.00 © 2007 American Chemical Society
Published on Web 12/14/2006

tronics and catalyst preparation. A more detailed description of the technique can be found elsewhere.[30]

Metal halides and ammonia are the primary ALD precursors for transition metal nitrides.[31−35] However, halide−ammonia processes require relatively high growth temperatures, and corrosive hydrogen halides are released. Thus, novel precursors for nitride ALD are being sought. Metal complexes containing alkylamido and alkylimido ligands have been introduced as potential precursors for transition metal nitrides. These novel precursors do not release aggressive side products, and deposition temperatures are lower than with metal halides. A wider range of substrate materials, including metals, can therefore be used. Amido−imido complexes of tantalum and tungsten have been synthesized and successfully used with ammonia as ALD precursors for the corresponding nitrides.[36,37] Bis(*tert*-butylimido)-bis(diethylamido)molybdenum has been used as a chemical vapor deposition (CVD) precursor for molybdenum nitride. However, the synthetic method for the precursor was not revealed.[38]

Until now, alkylamido- and alkylimido-based molybdenum complexes have not been studied as ALD precursors. Alkylamido−alkylimido-based precursors open up the possibility for new substrate materials and new applications for molybdenum nitride thin films. With amido−imido precursors, molybdenum nitride could be deposited on metal surfaces as protective coatings. In this paper, synthesis of a new molybdenum complex bis(*tert*-butylimido)-bis(dimethylamido)molybdenum and its potential as a precursor for ALD of molybdenum nitride are explored. Deposition tests were made on silicon, electrochemically grown nickel, chromium, and quartz glass. Nickel is a less-known substrate material in the ALD literature.[39] Deposited films were characterized for conformality, structure, and composition.

Experimental Section

Materials and Methods. All compounds were manipulated by the Schlenk technique in nitrogen atmosphere (99.999%, AGA) or in an inert atmosphere glovebox (Vacuum Atmospheres Co.). Acetonitrile was distilled over calcium hydride, and ether and hexane were distilled over sodium/benzophenone. All were degassed prior to use. Molybdenum(VI) dichloride dioxide (97% MoO_2Cl_2, Sigma-Aldrich) and lithium dimethylamide (95% $LiNMe_2$, Sigma-Aldrich) were used as received. *tert*-Butyl isocyanate (97% ^tBuNCO, Sigma-Aldrich) was degassed using a freeze-and-pump

Scheme 1. Route to the New Molybdenum Nitride Precursor, Bis(*tert*-butylimido)-bis(dimethylamido)molybdenum

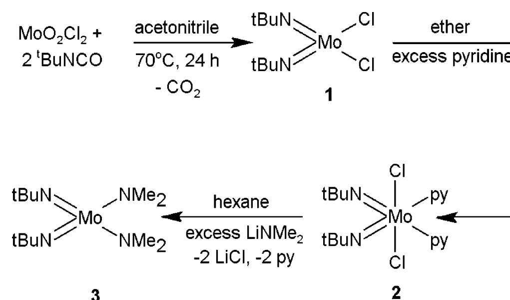

method. Pyridine (99.5%, Lab-Scan Analytical Sciences) was refluxed over calcium hydride, distilled, and degassed prior to use. The tungsten analogue, bis(*tert*-butylimido)-bis(dimethylamido)-tungsten, was synthesized via a published procedure.[37] When bis-(*tert*-butylimido)-bis(dimethylamido)tungsten became commercially available (Sigma-Aldrich), the commercial product was used in the depositions.

NMR spectra of intermediate and final products were collected with a Bruker Avance 250 MHz spectrometer. ^1H NMR spectra of $(^tBuN)_2MoCl_2$ (**1**) and $(^tBuN)_2MoCl_2(py)_2$ (**2**) were recorded in toluene-d_8 (99.5% D, Euriso-Top), and NMR data for $(^tBuN)_2Mo(NMe_2)_2$ (**3**) and its tungsten analogue $(^tBuN)_2W(NMe_2)_2$ (**4**) were collected in a glass capillary inside the NMR sample tube with $CDCl_3$ (99.5% D, Euriso-Top) used as lock solvent. Since compound **3** was found to be reactive toward chloroform, capillary setup was used to avoid chemical reactions between the sample and the solvent. Chemical shifts (ppm) are from TMS. C, H, and N analyses were performed with the EA 1110 CHNS-O microanalyzer from CE-Instruments.

Synthetic Procedure. The new molybdenum nitride precursor, bis(*tert*-butylimido)-bis(dimethylamido)molybdenum, $(^tBuN)_2Mo(NMe_2)_2$, was synthesized via the three successive reaction steps shown in Scheme 1.

Bis(*tert*-butylimido)-dichloromolybdenum(VI) (**1**) was synthesized via a published procedure.[40] To a solution of molybdenum-(VI) dichloride dioxide (4.88 g, 24.5 mmol) in acetonitrile (100 mL) was added *tert*-butyl isocyanate (4.9 mL, 49 mmol), and the mixture was heated at 70 °C for 24 h. Proton NMR was used to verify the structure of **1**.

The yellowish-brown suspension was allowed to cool to ambient temperature and was placed under vacuum to remove the solvent. To the brown residue, ether (100 mL) and excess pyridine (9.9 mL, 122.5 mmol) were added. The mixture was stirred overnight and placed under vacuum to remove ether and remaining pyridine. Synthesis of complex **2** has been reported previously, although the starting material was different. Chiu and co-workers used $MoCl_2(N^tBu)_2(dme)$ as a starting material. It was suspended in hexane, and pyridine was added to obtain **2**.[41] The structure of **2** was confirmed by proton NMR.

The yellow product of the second step was suspended in hexane (100 mL). Excess lithium dimethylamide (3.75 g, 73.5 mmol) suspended in hexane was slowly added to the mixture. The reaction is highly exothermic.

After overnight stirring the mixture was filtered through a Celite filtering medium to remove solid $LiNMe_2$ and LiCl. The solution was then placed under vacuum to remove hexane and pyridine.

(30) Leskelä, M.; Ritala, M. *Thin Solid Films* **2002**, *409*, 138.
(31) Ritala, M.; Leskelä, M.; Rauhala, E.; Haussalo, P. *J. Electrochem. Soc.* **1995**, *142*, 2731.
(32) Ritala, M.; Leskelä, M.; Rauhala, E.; Jokinen, J. *J. Electrochem. Soc.* **1998**, *145*, 2914.
(33) Hiltunen, L.; Leskelä, M.; Mäkelä, M.; Niinistö, L.; Nykänen, E.; Soininen, P. *Thin Solid Films* **1988**, *166*, 149.
(34) Alén, P.; Ritala, M.; Arstila, K.; Keinonen, J.; Leskelä, M. *J. Electrochem. Soc.* **2005**, *152*, G361.
(35) Juppo, M.; Ritala, M.; Leskelä, M. *J. Electrochem. Soc.* **2000**, *147*, 3377.
(36) van der Straten, O.; Zhu, Y.; Dunn, K.; Eisenbraun, E. T.; Kaloyeros, A. E. *J. Mater. Res.* **2004**, *19*, 447.
(37) Becker, J. S.; Suh, S.; Wang, S.; Gordon, R. G. *Chem. Mater.* **2003**, *15*, 2969.
(38) Sun, S.-C.; Chiu, H.-T. U.S. Patent 6,114,242, 2000.
(39) Wank, J. R.; George, S. M.; Weimer, A. W. *J. Am. Ceram. Soc.* **2004**, *87*, 762.
(40) Schoettel, G.; Kress, J.; Osborn, J. A. *J. Chem. Soc., Chem. Commun.* **1989**, 1062.
(41) Chiu, H.-T.; Chang, G.-B.; Ho, W.-Y.; Chuang, S. H.; Lee, G. H.; Peng, S.-M. *J. Chin. Chem. Soc.* **1994**, *41*, 755.

From this residue the product was distilled under reduced pressure (72 °C, 8 Torr). The new molybdenum nitride precursor, bis(*tert*-butylimido)-bis(dimethylamido)molybdenum (2.594 g, 8.0 mmol, yield 33% based on MoO_2Cl_2) is an orange, highly air-sensitive liquid, which should be stored and handled under inert atmosphere. Yields reported in the literature for syntheses of transition metal amido−imido complexes are usually below 50%, typically around 40%.[37,42−44] ^{1}H NMR results for **3**: 2.14 ($NC(CH_3)_3$, singlet, 18 protons), 4.17 ($N(CH_3)_2$, s, 12). $^{13}C\{^1H\}$ NMR for **3**: 34.0 (six carbons), 54.9 (4), 68.3 (2). Elem composition. Calcd for $C_{12}H_{30}N_4$-Mo: C, 44.2; H, 9.3; N, 17.2; Mo, 29.4. Found: C, 44.4; H, 9.6; N, 17.6. For comparison, NMR analyses in the glass capillary were also made for the tungsten analogue **4**. ^{1}H NMR results for **4**: 1.78 ($NC(CH_3)_3$, singlet, 18 protons), 3.91 ($N(CH_3)_2$, s, 12). $^{13}C\{^1H\}$ NMR for **4**: 34.6 (six carbons), 54.2 (4), 66.6 (2).

The effect of pyridine ligands on the chlorine−molybdenum bonding in complexes **1** and **2** was studied by density functional theory (DFT) at the B3LYP level and LANL2DZ as the basis set. There is a little structural information available for complex **1**. Full structural optimization was performed for both complexes. Calculations were done by the Gaussian 03 program package.[45]

Calorimetric Studies. Differential scanning calorimetry (DSC) studies were carried out to find the self-decomposition temperature with a Mettler Toledo DSC821e differential scanning calorimeter. A sample of bis(*tert*-butylimido)-bis(dimethylamido)molybdenum (1.388 mg) was loaded, in an inert atmosphere glovebox, into a 30-μL reusable high-pressure crucible. DSC data were collected between 25 °C and 350 °C. A sample of the tungsten analogue, bis(*tert*-butylimido)-bis(dimethylamido)tungsten (**4**; 5.374 mg), was loaded in the same manner and measured in the temperature range 25−400 °C. Sample crucibles were weighed before and after DSC measurement in order to trace possible leakage. In both cases the heating rate was 5 °C/min.

ALD of Molybdenum Nitride. ALD tests were carried out with a reactor system constructed in-house inside an ASM Microchemistry F-120 reactor body. The reactor system schematics are shown in Figure 1. Nitrogen (99.999% N_2, AGA) was purified by leading it through an alumina column (Figure 1, n) and a Mykrolis inert gas purifier (model WPMV200SI) (Figure 1, m). Ammonia (99.98% NH_3, AGA) was dried and purified in a similar way by passing it through an alumina column and Mykrolis gas purifier (model WPMV200SM). Nitrogen is fed to the valve collar where valves direct the flow to the selected source tube. Total pressure inside the reactor was on the order of 10 mbar during depositions, ammonia flow was 100 standard cubic centimeters (sccm), and nitrogen flow was 400 sccm. Hence, the partial pressure of ammonia is 2.0 mbar, and the concentration is 20% in volume. The deposition temperature varied from 210 °C to 330 °C, while the evaporation temperature of the metal precursors was 40 °C. Metal precursors were loaded into the reactor with a syringe-tap-needle system in an air-sensitive manner (Figure 1, d). The syringe was loaded with the precursor in a glovebox, closed with the tap, taken out from the glovebox, and connected to another tap in the valve collar outside the reactor system under nitrogen flow. With the reactor system at atmospheric pressure, the metal precursor was injected to the evaporation vessel (Figure 1, a) through the needle. Both taps were then closed, and the reactor system was driven to a deposition pressure of 10 mbar.

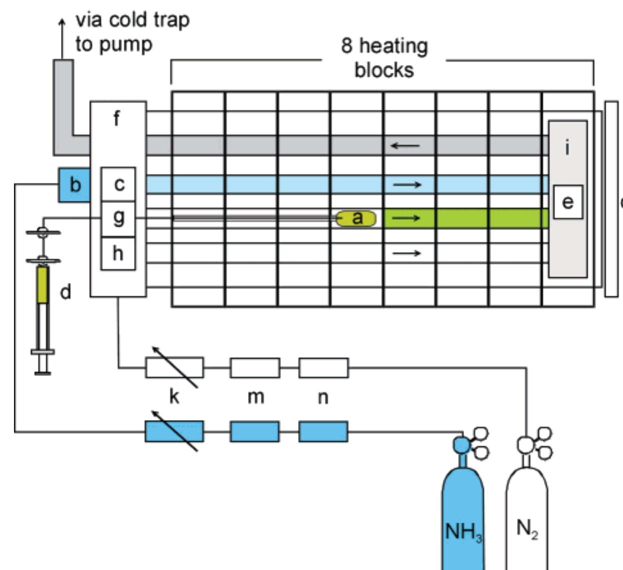

Figure 1. ALD reactor system schematics: evaporation vessel for metal precursor (a), pulsing valve for ammonia (b), pulsing valve for nitrogen (carrier of ammonia; c), syringe-tap-needle system for air-sensitive metal precursor loading (d), substrate (e), valve collar (f), pulsing valve for nitrogen (carrier of metal precursor; g), pulsing valve for nitrogen (purge; h), reactor space (i), mass flow controllers (k), gas purifiers (m), alumina columns for drying (n), and connection to nitrogen atmosphere glovebox (o).

Depositions were successfully made on silicon, chromium, quartz glass, and electrochemically grown nickel. Substrates were cleaned with chloroform to remove any traces of organic contaminants and with 1% sulfuric acid to remove inorganics. Finally, substrates were rinsed with deionized water and blown dry with dry pressurized air. Substrates were inserted to the reactor chamber via the glovebox connection (Figure 1, o).

The deposition cycle consists of the following steps: (1) metal precursor pulse by opening valve g on Figure 1, (2) purge by opening valve h, (3) ammonia pulse by opening valves b and c, and (4) purge by opening valve h. Purge periods were set at 5 s, metal precursor pulse time was varied between 1 and 6 s, and ammonia pulse time was varied between 2 and 6 s. Blank deposition (ammonia pulse 0 s) was executed to discover any CVD character in the growth. After deposition, the reactor system was restored to atmospheric pressure, and coated substrates were removed via the connection to the glovebox (Figure 1, o) to minimize air contamination to the reactor.

Film Characterization. Film thicknesses were determined by variable angle spectroscopic ellipsometry (J.A. Woollam). The Lorentz oscillator model was applied for modeling optical properties of nitride films. Scanning electron microscopy (Hitachi S-4800) was used to characterize film morphology and conformality. Film composition and elemental depth profile were determined by time-of-flight elastic recoil detection analysis (TOF-ERDA) in the

(42) Chiu, H.-T.; Lin, J. C.; Chuang, S.-H.; Lee, G.-H.; Peng, S.-M. *J. Chin. Chem. Soc.* **1998**, *45*, 355.
(43) Chiu, H.-T.; Chuang, S.-H.; Tsai, C.-E.; Lee, G.-H.; Peng, S.-M. *Polyhedron* **1998**, *17*, 2187.
(44) Danopoulos, A. A.; Leung, W.-H.; Wilkinson, G.; Hussain-Bates, B.; Hursthouse, M. B. *Polyhedron* **1990**, *9*, 2625.
(45) Frisch, M. J.; Trucks, G. W.; Schlegel, H. B.; Scuseria, G. E.; Robb, M. A.; Cheeseman, J. R.; Montgomery, J. A., Jr.; Vreven, T.; Kudin, K. N.; Burant, J. C.; Millam, J. M.; Iyengar, S. S.; Tomasi, J.; Barone, V.; Mennucci, B.; Cossi, M.; Scalmani, G.; Rega, N.; Petersson, G. A.; Nakatsuji, H.; Hada, M.; Ehara, M.; Toyota, K.; Fukuda, R.; Hasegawa, J.; Ishida, M.; Nakajima, T.; Honda, Y.; Kitao, O.; Nakai, H.; Klene, M.; Li, X.; Knox, J. E.; Hratchian, H. P.; Cross, J. B.; Bakken, V.; Adamo, C.; Jaramillo, J.; Gomperts, R.; Stratmann, R. E.; Yazyev, O.; Austin, A. J.; Cammi, R.; Pomelli, C.; Ochterski, J. W.; Ayala, P. Y.; Morokuma, K.; Voth, G. A.; Salvador, P.; Dannenberg, J. J.; Zakrzewski, V. G.; Dapprich, S.; Daniels, A. D.; Strain, M. C.; Farkas, O.; Malick, D. K.; Rabuck, A. D.; Raghavachari, K.; Foresman, J. B.; Ortiz, J. V.; Cui, Q.; Baboul, A. G.; Clifford, S.; Cioslowski, J.; Stefanov, B. B.; Liu, G.; Liashenko, A.; Piskorz, P.; Komaromi, I.; Martin, R. L.; Fox, D. J.; Keith, T.; Al-Laham, M. A.; Peng, C. Y.; Nanayakkara, A.; Challacombe, M.; Gill, P. M. W.; Johnson, B.; Chen, W.; Wong, M. W.; Gonzalez, C.; Pople, J. A. *Gaussian 03*, revision C.02; Gaussian, Inc.: Wallingford, CT, 2004.

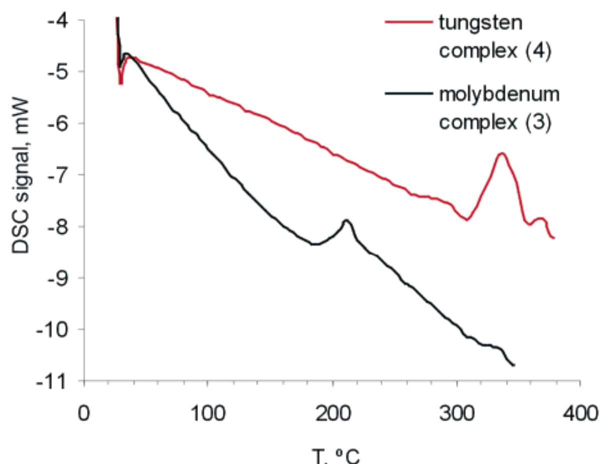

Figure 2. DSC plots for the new molybdenum complex **3** and its tungsten analogue **4**.

Accelerator Laboratory, University of Helsinki. Powder X-ray diffraction (XRD) studies were made by the Philips MPD 1880 instrument (Helsinki University of Technology) by $\theta-2\theta$ scan and using Cu Kα radiation.

Results and Discussion

Synthesis. A straightforward synthetic route (Scheme 1) is introduced for bis(*tert*-butylimido)-bis(dimethylamido)-molybdenum (**3**), a new molybdenum nitride ALD precursor. Without the second step (addition of pyridine) and also when addition of $LiNMe_2$ was done at −60 °C, the synthesis produced very low yields of **3**. Pyridine coordination to molybdenum increases the electron density around molybdenum which increases the molybdenum−chlorine bond length. A DFT study revealed a clear difference in Mo−Cl bond lengths: for $(^tBuN)_2MoCl_2$ (**1**), 2.39 Å, and for $(^tBuN)_2MoCl_2(py)_2$ (**2**), 2.53 Å. The increment in the bond length indicates weaker molybdenum−chlorine bonding, and reactivity of the complex **2** toward lithium dimethylamide is therefore higher.

Likewise, excess of $LiNMe_2$ appears to be essential. When stoichiometric amounts of lithium reagent were used, only 15% yields of **3** were obtained. Both lithium dimethylamide and complex **2** have limited solubility in hexane, which reduces the rate of reaction compared to the situation where both of the components are dissolved. The reaction between complex **2** and lithium dimethylamide is very exothermic, as was noticed. The low solubility of reagents and resulting low reaction rate keeps the reaction temperature in controllable limits, but on the other hand to get reasonable yields in reasonable time, excess of lithium reagent has to be used.

DSC Studies. The self-decomposition temperatures of **3** and its tungsten analogue **4** were determined by DSC to find the maximum ALD growth temperatures. The DSC plots of **3** and **4** are presented in Figure 2.

The exothermal signal sets in at 190 °C for molybdenum complex **3** and at 310 °C for the tungsten analogue. These are as one would expect for maximum deposition temperatures in self-limiting growth. Earlier, self-limiting tungsten nitride ALD growth with the tungsten complex was reported to take place below 350 °C.[37] The slope in the baseline is induced by a mass difference between sample and reference crucibles.

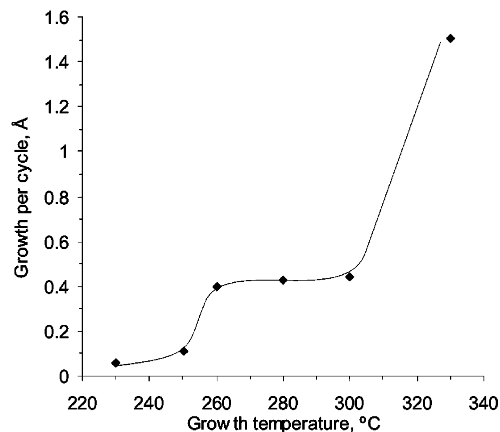

Figure 3. Molybdenum nitride film growth per deposition cycle.

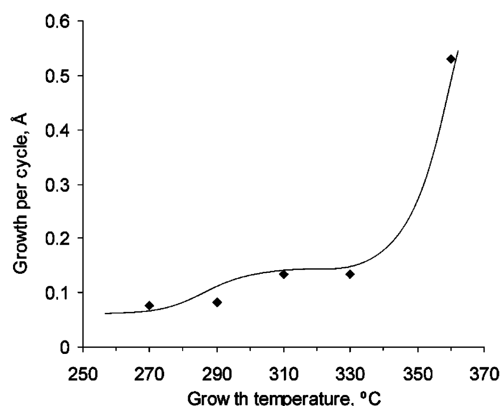

Figure 4. Tungsten nitride film growth per deposition cycle.

Depositions. The optimum temperature range for ALD was determined by varying the growth temperature and determining the film growth per cycle. The pulse times and the purge time were fixed at 5 s. Precursor evaporation temperature was set at 50 °C. Growth per cycle as a function of deposition temperature is shown in Figure 3. The deposition temperature window was also explored for the tungsten analogue (Figure 4). The precursor evaporation temperature was 40 °C, and the precursor pulse time was 2 s. The ammonia pulse and purge times were set at 5 s.

The ALD growth window for molybdenum nitride was found to be 260−300 °C. This is lower than that reported earlier.[33,34] The temperature window for tungsten nitride growth was 290−340 °C. Growth per cycle (Figure 4) was lower than Becker et al.[37] have reported, most probably because tungsten precursor pulse time and evaporation temperature were not optimized here.

For both precursors, higher temperatures than expected from the DSC data were found to be suitable for atomic layer growth. In the DSC sample pan, precursor decomposition takes place at high pressure, whereas in the ALD reactor the pressure is on the order of 10 mbar. Reaction side products can cause autocatalysis at high pressure and shift the reaction to lower temperatures.

For molybdenum nitride depositions, the growth temperature was set at 280 °C to achieve maximum ALD growth per cycle. In an attempt to find the optimum pulse time for maximum growth per cycle, pulse times were varied, with ammonia between 0 and 7 s and with the molybdenum

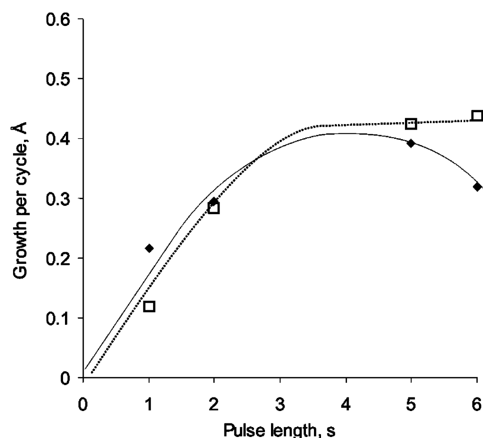

Figure 5. Growth per cycle as a function of molybdenum precursor pulse time: ammonia pulse and purge times were fixed at 5 s, and deposition temperature was fixed at 280 °C. Two precursor evaporation temperatures were used, 40 °C (◆, solid line) and 50 °C (□, dotted line).

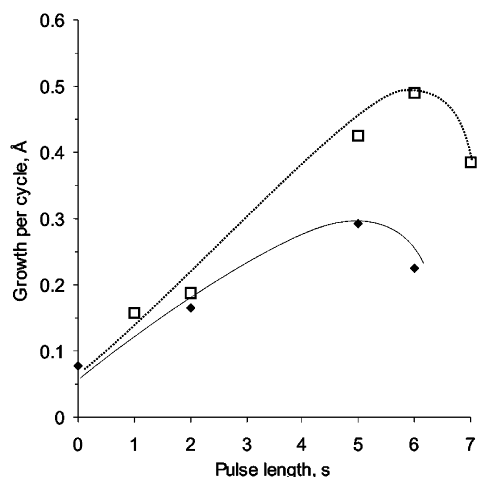

Figure 6. Growth per cycle as a function of ammonia pulse time: Mo precursor pulse time was fixed at 5 s, purge time was fixed at 5 s, and deposition temperature was fixed at 280 °C. Two precursor evaporation temperatures were used, 40 °C (◆, solid line) and 50 °C (□, dotted line).

precursor between 1 and 6 s. Results for these experiments are presented in Figures 5 and 6.

For the molybdenum precursor, maximum growth per cycle was achieved with a 5 s pulse, and for ammonia it was acheived with a 6 s pulse. The transition point seen in both curves in Figure 6 is probably induced by thermal decomposition of the adsorbed precursor complexes, as the pulse time is relatively long compared to other ALD systems found in the literature. In most cases the pulse times are kept below 2 s with a F-120 type reactor.[31,32] Also the concentration of ammonia and resulting molar dose are an order of magnitude higher than reported with halide based nitride processes.[31,34] In the case of the analogous tungsten nitride process, Becker et al. reported that saturation of the ammonia pulse required over 10^4 times the dose compared to the corresponding saturative tungsten precursor dose. Becker et al. also discussed that rather than reacting with the surface species of the metal precursor, ammonia could act as a catalyst.[37] In the tungsten nitride process, however, no reduction in the growth rate as a function of ammonia pulse length was observed. Yet, in the molybdenum nitride case reported here, ammonia could further catalyze the surface reaction and decompose the surface species resulting in

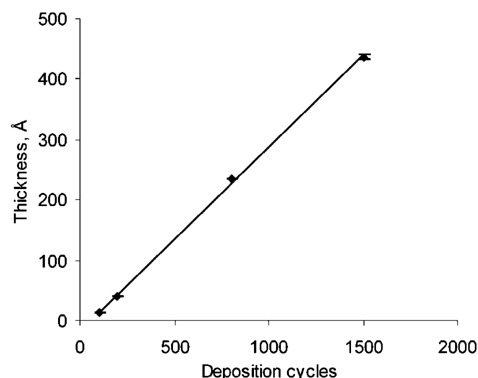

Figure 7. Linear growth of molybdenum nitride film as a function of number of deposition cycles.

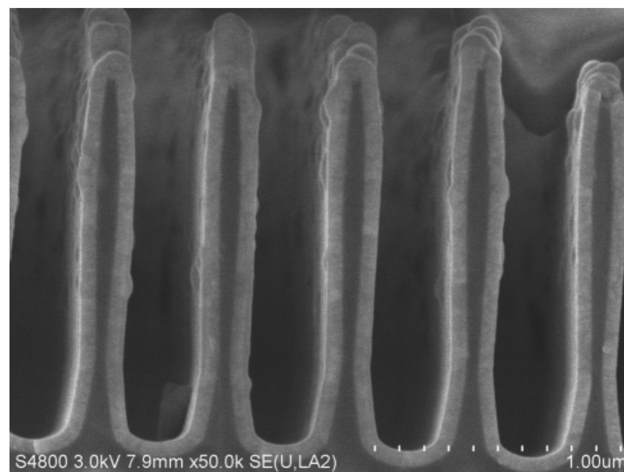

Figure 8. Cross section of 70-nm molybdenum nitride film deposited on quartz (1600 cycles, precursor, ammonia and purge pulses 5 s, growth temperature 280 °C, precursor evaporation temperature 40 °C).

reduction in the growth rate as the ammonia pulse is elongated. As the adsorbed precursors decompose, the number of active sites decreases, and so does the growth per cycle.

Decrease in the growth per cycle as a function of pulse time can also be seen in Figure 5 in the case of the molybdenum precursor. This can be also a result of precursor decomposition on the surface, but most likely the effect is caused by a too dilute precursor vapor and too low of a precursor evaporation temperature. A low deposition rate was also found in deposition tests without ammonia (pulse sequence: 2 s Mo precursor pulse, 5 s purge pulse), which indicates minor CVD growth.

Linearity of the growth was studied by varying the number of deposition cycles between 100 and 1500. The molybdenum precursor pulse time was fixed at 2 s, the ammonia pulse time was fixed at 5 s, and the deposition temperature was fixed at 280 °C. As can be seen in Figure 7, good linearity was obtained, with a squared linear correlation factor of 0.9992.

Film morphology and conformality were studied by scanning electron microscopy. Deposited films were smooth, and film conformality was good within the tested aspect ratios. A cross section of the patterned quartz substrate with 70 nm deposited molybdenum nitride film is presented in Figure 8. The aspect ratio of the pattern was 3.8, and the conformality of the film was 98%.

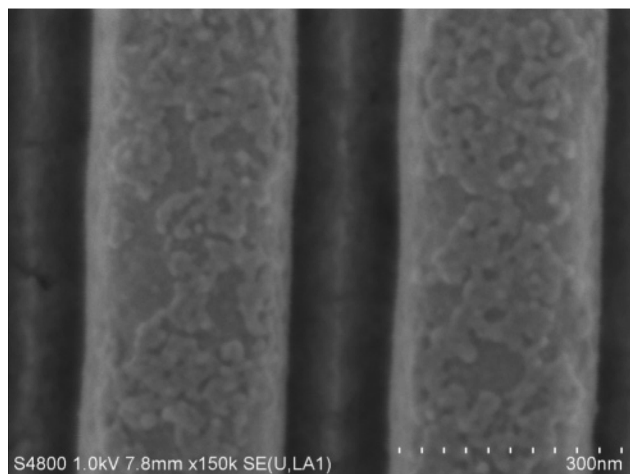

Figure 9. Patterned nickel substrate, structure depth 800 nm.

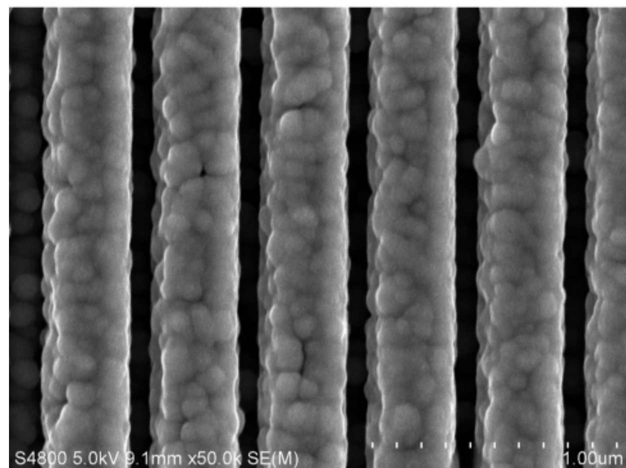

Figure 10. Molybdenum nitride (65 nm) on patterned nickel (1500 cycles, all pulses 5 s, deposition temperature 280 °C, precursor evaporation temperature 40 °C).

Molybdenum nitride was also successfully deposited on patterned electrochemically grown nickel. Films were conformal, and growth rate per cycle was the same as with silicon and quartz substrates. The grainy structure of the nitride film is caused by irregularities on the nickel substrate. The blank patterned nickel substrate is presented in Figure 9, and a 65-nm molybdenum nitride film on nickel is presented in Figure 10. This is one of the few examples where nickel has been used as an ALD substrate material.[39]

The patterned silicon substrate with a chromium etch mask was used as a substrate to compare deposition rates on metallic and silicon substrates. As can be seen in Figure 11, the growth rate per cycle (0.4 Å) for the molybdenum nitride film is the same on chromium and silicon. Step coverage (film thickness on groove wall divided by the film thickness on flat surface) was 94%.

XRD was measured at Helsinki University of Technology by the Philips MPD 1880 instrument. Collected data of the as-deposited and the annealed films (650 °C, 30 min under N_2 atmosphere) are presented in Figure 12. According to XRD data, films seem to be mostly amorphous, since diffraction peaks are weak and broadened. Reflections at 2.38, 2.27, and 2.07 can be indexed to (112), (103), and (200) reflections of the tetragonal β-Mo_2N phase, respectively.[46] Annealing has a minor crystallizing effect on the film, since the intensity increases and full width at half-maximum values decreases during annealing.

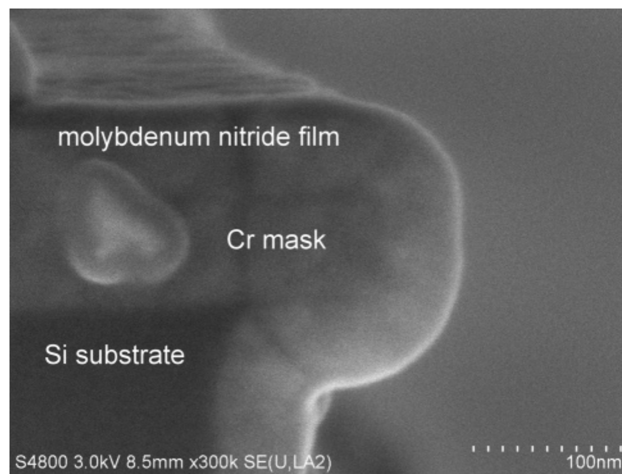

Figure 11. Molybdenum nitride (65 nm) on patterned silicon with chromium etch mask (1500 cycles, all pulses 5 s, deposition temperature 280 °C).

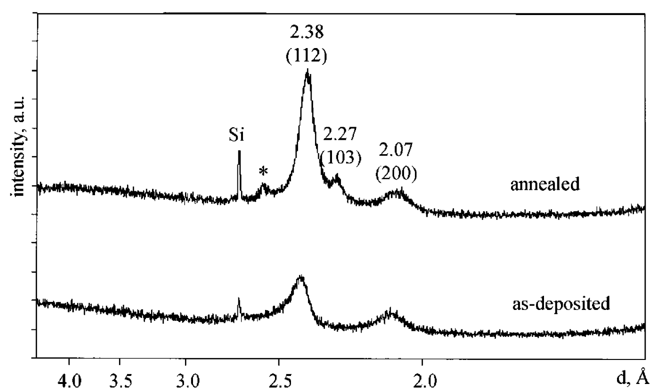

Figure 12. XRD patterns of the as-deposited and the annealed molybdenum nitride film. Crystalline phase is indexed as tetragonal β-Mo_2N. Reflection denoted with * represents MoO_3.[47]

Table 1. Elemental Proportion of a 44 nm Molybdenum Nitride Film on Silicon

element	atomic percentage	error
Mo	38	2
N	35	3
O	15.5	1.4
C	4.7	0.7
H	6.9	0.6

Film composition and the elemental depth profile were determined by TOF-ERDA (Accelerator Laboratory, University of Helsinki). The elemental composition for a 44-nm film is presented in Table 1. The precursor pulse time was 2, the ammonia pulse time was 5, and the purge time was 5 s. The deposition temperature was set at 280 °C, and the number of deposition cycles was set at 1500. According to TOF-ERDA data, the elemental distribution was uniform throughout the film thickness.

The crystalline phase observed in XRD corresponds to a molybdenum to nitrogen ratio of 2. However, the proportion of molybdenum and nitrogen contents in the film is close to

(46) Joint Committee on Powder Diffraction Standards, Card 24-768.

one. This indicates a nitrogen rich amorphous phase in the film. Similar consistency of ALD molybdenum nitride thin films has been previously reported. Alén and co-workers used molybdenum pentachloride and ammonia as precursors, and the crystalline phase was characterized as cubic γ-Mo_2N, but the overall elemental composition ratio of molybdenum and nitrogen was close to one.[34] Noticeably, molybdenum to nitrogen ratio in the film seems to be independent from the precursor system used.

Oxygen contamination is a well-known problem in ALD nitride thin films.[31,32,48] In the case of titanium nitride Ritala et al. suggested three possible ways for oxygen incorporation into the film. Oxygen can contaminate the film from oxygen and/or moisture residues in carrier and reactant gases both during the film growth and within a cooling period or from ambient air after the film is taken out from the reactor. Ritala et al. also found that the thinner the film, the higher the oxygen content in the film.[31] In this study, the air exposure is minimized by handling the substrates via glovebox connection and by cleaning the gases with the chemical purifiers. Oxygen can however contaminate the film after the thin film sample is brought out from the glovebox and exposed to ambient air.

Conclusions

A synthetic procedure is presented for a new molybdenum complex, bis(*tert*-butylimido)-bis(dimethylamido)molybdenum. The structure of the new complex was determined by NMR and elemental analysis, and the results of the analyses were compared with those for the tungsten analogue. DSC studies were carried out to determine the self-decomposition temperature, in other words, the maximum ALD growth temperature. Suitable parameters for ALD of molybdenum nitride from bis(*tert*-butylimido)-bis(dimethylamido)molybdenum and ammonia precursors were identified. The optimum temperature range for the deposition was 260−300 °C, which is lower than temperatures for molybdenum nitride ALD reported earlier. Importantly, the emission of aggressive hydrogen halides is avoided, which enables the use of a wider range of substrate materials and opens new applications for molybdenum nitride, protective coatings as an example. Depositions were successfully accomplished on silicon, quartz, chromium, and nickel with 0.5 Å maximum growth per cycle. The growth per cycle was maintained over different substrate materials. These findings suggest that amido−imido type transition metal complexes have more versatile surface chemistry than previously reported halide-based ALD nitride precursors. Deposited films had high conformality of 98%. The deposited films were mainly amorphous including a tetragonal β-Mo_2N phase.

Acknowledgment. Funding was provided by the European Union and the Employment and Economic Development Centre for North Karelia. The authors are grateful to Prof. Markku Kuittinen and Mr. Samuli Siitonen, Department of Physics, University of Joensuu, for providing the substrates for deposition tests. Ms. Taina Nivajärvi performed the elemental analyses.

CM0620279

(47) Joint Committee on Powder Diffraction Standards, Cards 21-569 and 5-508.
(48) Ritala, M.; Asikainen, T.; Leskelä, M.; Jokinen, J.; Lappalainen, R.; Utriainen, M.; Niinistö, L.; Ristolainen, E. *Appl. Surf. Sci.* **1997**, *120*, 199.